Asian Journal of Engineering and Applied Technology
ISSN: 2249-068X (P) Vol. 3 No. 2, 2014, pp.63-67

DOI: https://doi.org/10.51983/ajeat-2014.3.2.713

Influence of Zinc Substitution on Physicochemical and In-vitro Behaviour of Nanodimensional Hydroxyapatite

Suchita Kohli [1*], Uma Batra [2] and Seema Kapoor [1]

[1]Dr. SSBhatnagar University Institute of Chemical Engineering &Technology, Panjab University, Chandigarh, India
[2]Department of Materials & Metallurgical Engineering, PEC University of Technology, Chandigarh, India
* *corresponding author e-mail*: suchita_kohli@yahoo.co.in
(Received 1 October 2014; Revised 26 October 2014; Accepted 16 November 2014; Available online 24 November 2014)

Abstact - Hydroxyapatite has widely been used as bone substitute due to its good biocompatibility and bioactivity. In the present work, hydroxyapatite was substituted with Zinc (Zn) to improve its bioactivity. The study reports the technique to synthesize nanodimensional pure HA (HA) and Zn substituted HA (ZnHA) powders (with Zn in the range of 2-15 mol%) using sol-gel technique and the influence of Zn on physicochemical and in-vitro behavior of HA. The morphology and size of nanopowders were characterized by transmission electron microscopy (TEM). The BET surface area was evaluated from N_2 adsorption isotherms. Structural analysis was investigated by means of x-ray diffraction (XRD) and Fourier transform infrared spectroscopy (FTIR). In-vitro study of nanopowders was assessed upto 30 days in simulated body fluid (SBF) maintained at 37 °C. TEM micrographs showed that synthesized HA and ZnHA powders were nanodimensional. HA as well as ZnHA powders (with 2 and 10 mol% Zn) had regular shapes whereas ZnHA powders (with 5 and 15 mol% Zn) had irregular and formed agglomerates. BET surface areas of ZnHA (with 2 and 10 mol% Zn) were higher as compared ZnHA (with 5 and 15 mol% Zn). The XRD and FTIR results revealed that an increase in Zn amount affects the phase composition, crystallization and structural parameters of HA. ZnHA powders exhibited more bioactive behavior than HA.

Keywords: Hydroxyapatit, Zinc Substitution, Nanopowders, BET Surface Area, Bioactivity.

I.INTRODUCTION

Hydroxyapatite (HA, $Ca_{10}(PO_4)_6(OH)_2$) constitutes the mineral phase of bone. It has been widely used as bone filler, aesthetic restorative, coating of orthopedic implants and filler of inorganic/polymer composites [1], due to its obvious properties of biocompatibility, bioactivity, osteoconductivity, non toxicity and non inflammatoriness. But there is a significant difference of properties between biological apatite found in the bone mineral and conventional synthetic HA. The biological apatite differs from synthetic HA in several aspects including nonstoichiometry, low degree of crystallinity and small crystal size. It contains several cationic substitutions like, Zn^{2+}, Na^{+}, Mg^{2+}, K^{+} , Mn^{2+} etc [2]. Among these cations, Zn^{2+} has drawn considerable attention of the researchers as it is capable of increasing osteoblast proliferation, biomineralization and bone formation [3, 4]. It is also involved in various metabolic mechanisms for the normal growth and development of bone and its deficiency is associated with decrease in bone density [5, 6]. Its incorporation into HA lattice inhibit crystal growth as well thermal stability [7, 8] and modulates morphology and crystallinity of crystals [9].

LeGeros et al. [10] reported that the incorporation of a small amount of Zn^{2+} into the HA structure induces an evident reduction in the degree of crystallinity of the apatitic phase, which leads to the inability of the structure to host greater amounts of Zn. They also reported that the substitution of Zn for Ca increased the apatite lattice parameters a and c [11]. Miyaji et al. [12] synthesized Zn-substituted HA by the precipitation method and reported that maximum of 15 mol.% of Zn can be substituted in HA. Hayakawa et al. [13] prepared Zn-containing HA particles by an ion-exchange reaction process and have reported that there is decrease in lattice parameters with an increase in Zn content. However their study was limited upto 3 mol.% Zn. Li et al. [14] prepared Zn-substituted HA powders by a hydrothermal method and reported that the lattice parameter a decreased upto 10 mol.% Zn beyond which it increased, whereas the lattice parameter c decreased with increase in Zn mol.%.

The previous studies do not provide any direct evidence of the partial substitution of Ca by Zn in the apatite lattice. It is reported that Zn is adsorbed on the surface of HA or is present in the amorphous phase. The structural changes to the apatites on Zn substitution have been reported only by few researchers [12, 15]. In the present work, the effect of addition of Zn on physicochemical and bioactivity behaviour of HA has been investigated in the range 2- 15 mol% Zn.

II.MATERIALS AND METHODS

Synthesis of HA and ZnHA Nanopowders

Nanodimensional HA powder was synthesized by sol-gel route using calcium nitrate tetrahydrate (CNT, Merck, Germany) and potassium di-hydrogen phosphate (KDP, Merck, Germany). 1.0 M solution of CNT and 0.6 M solution of KDP in deionised water was taken in such amounts that Ca/P molar ratio was maintained at 1.67. CNT was added drop by drop gradually to KDP under vigorous stirring using mechanical stirrer (2500 rpm) for one hour. The pH of the solution was maintained at 10 with addition of ammonia solution. In case of nanodimensional ZnHA powders, zinc nitrate tetrahydrate (ZNT) was added to CNT with varying amounts of zinc i.e 2%, 5%, 10% and 15%. (Ca+Zn)/P molar ratio was maintained at 1.67. Gels were obtained and were aged at room temperature for 24 hours. Gelatinous precipitates formed were filtered by a centrifuge and washed thoroughly by distilled water. The precipitates were dried

in an oven at 70 °C for 24 h and the powders were prepared by crushing them.

Powder Characterization

The elemental molar composition of nanopowders was studied by using wavelength dispersive X-ray Fluorescence (WD-XRF, Model: S8 TIGER, Make Bruker, Germany). The nanopowders (about 8 gm) were pressed to pellets with 34 mm diameter and 1.5 mm thickness under 15 tons pressure using hydraulic press. The pellets were analyzed for atomic concentrations of Ca, P and Zn content in the energy dispersive spectra of 0-60 Kev. XRF patterns were obtained for ZnHA2, ZnHA5, ZnHA10 and ZnHA15 nanopowders, respectively.

Transmission Electron Microscope (TEM) (Hitachi, 7500) with resolution of 0.2 nm, operated at an accelerating voltage of 80-100 KV was used for observing morphology and size of nanopowders. The powders were ultrasonically dispersed in ethanol to form a dilute suspension and then a drop of suspension was dropped on carbon coated copper grid of 300 mesh for observation.

The BET surface area of powders was evaluated by N_2 adsorption using Quantachrome Instruments NOVA 2200e Surface Area Analyser using Brunauer–Emmett–Teller (BET) method [16]. The linearized form of BET equation is expressed by:

$$\frac{p}{v(p_o - p)} = \frac{1}{v_m z} + \frac{z-1}{v_m z}\frac{p}{p_o} \qquad (1)$$

where p/p_0 is the relative vapour pressure of the adsorbate, v is the volume of gas adsorbed, v_m is the volume of gas adsorbed in a monolayer, and z is a constant related to the energy of adsorption. The minimum relative pressure p/p_0 resolution was 2 x 10^{-5}. A linear regression of the left side of BET equation and p/p_0 yields a slope and intercept from which z and v_m are obtained. The BET surface area is then calculated from v_m [17].

X-ray diffraction (XRD, Philips X'Pert 1710) analysis was performed for all powders using Cu Kα radiation, λ = 1.54 Å, 2θ- 20° to 80°, step size 0.017°, time per step 20.03 s, and scan speed 0.005 °/s. Relative amount of different phases present in nano-powders were estimated on the basis of the peak intensity variation by means of external standard method. Both cell parameters, a and c have been calculated using the equation given below [18]:

$$\frac{1}{d^2} = 4/3\left[\frac{h^2 + hk + k^2}{a^2}\right] + \frac{l^2}{c^2} \qquad (2)$$

where d is the distance between adjacent planes in the set of Miller indices (h k l), the reference for HA being JCPDS file no. 09-0432 (a = 9.418 Å, b = 9.418 Å, c = 6.884 Å, space group p63/m).

Infrared spectra (FTIR Perkin Elmer) were recorded in the region 400–4000 cm^{-1} using KBr pellets (1% wt/wt), with spectral resolution of 2 cm^{-1}, taking four scans for each sample. The in-vitro behavior of the nanopowders was studied by immersing the nanopowders in simulated body fluid (SBF or Kokubo solution) stored in polystyrene bottles and placed in a biological incubator at 36.5 °C for 30 days. SBF was prepared in double ionized distilled water using various reagents as described earlier [19]. The pH of the solution was measured at an interval of 5 days using digital pH meter.

III.RESULTS AND DISCUSSION

Chemical Composition ZnHA nanopowders

XRF provided the quantitative composition of the synthesized ZnHA powders. The relative amounts of calcium (Ca), zinc (Zn) and phorophous (P) determined from XRF patterns are given in Table 1.

TABLE 1. CHEMICAL COMPOSITION OF ZNHA NANOPOWDERS FROM XRF

Sample	Mol. % of Zn added during synthesis	Mol. % in synthesized nanopowders			Zn/(Ca +Zn)	Ca/P	(Ca+Zn)/P
		Ca	Zn	P			
ZnHA2	2.0	61.7	0.871	37.4	1.4	1.65	1.676
ZnHA5	5.0	60.38	1.82	37.7	2.9	1.60	1.668
ZnHA10	10.0	58.88	3.832	37.28	6.1	1.58	1.682
ZnHA15	15.0	54.6	8.2	37.18	13.1	1.47	1.689

The presence of Zn was confirmed in all ZnHA nanopowders though its concentration was lesser than corresponding initial addition of Zn mol.% during synthesis. The stoichiometric HA has Ca/P molar ratio of 1.67. Since Zn is likely to replace Ca ions, the stoichiometry of ZnHA nanopowders was compared with (Ca+Zn)/P molar ratios. On increasing the Zn from 2 to 15 mol.%, Ca/P ratio decreased from 1.67 to 1.47, thus affecting the stoichiometry of HA nanopowder. Thus Zn substitution might have occurred for Ca sites in the HA structure. The (Ca+Zn)/P ratio of ZnHA2 and ZnHA5 was closer to the ratio for HA, whereas it was higher in case of ZnHA10 and ZnHA15 nanopowders. This might be due to the fact that most of the Zn^{2+} ions substituted the position of Ca^{2+} in the HA lattice for ZnHA2 and ZnHA5, whereas in ZnHA10 and ZnHA15, it might be present as any other phase of Zn outside the HA lattice, as is also reported by Ren et al. [15].

Microstructure and BET Surface Area of Nanopowders

The particles morphology of HA and ZnHA nanopowders were determined by TEM micrographs shown in Fig. 1 (a and b), respectively. The size of the nanopowders is given in Table 2. ZnHA2 and ZnHA10 consisted of nanodimensional flake-like particles, whereas ZnHA10 exhibited relatively smaller size. ZNHA5 and ZnHA15 powders showed agglomeration.

TABLE 2. MOROPHOLOGY AND SIZE RANGE OF HA AND ZNHA NANOPOWDERS

Sample		HA	ZnHA2	ZnHA5	ZnHA10	ZnHA15
Moropholo gy		Flake like				
Size range (nm)	L	28-40	26-36	18-24	15-26	10-20
	D	8-14	6-12	2-3	5-7	2-3

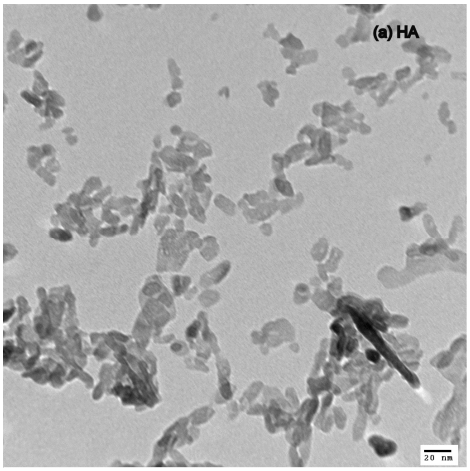

(a)

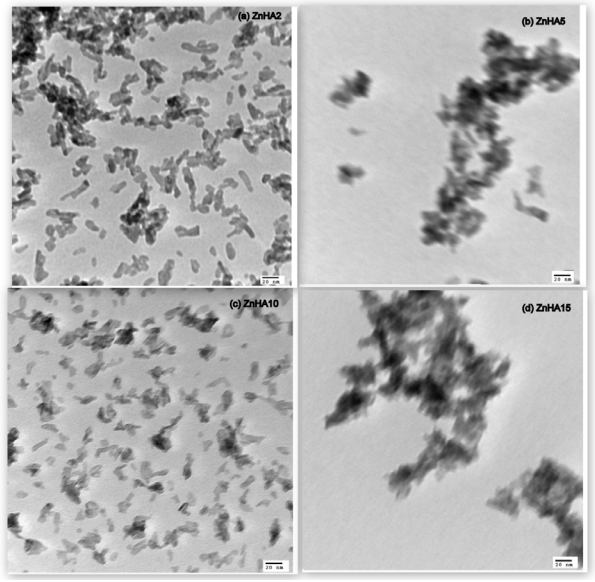

(b)

Fig. 1. TEM micrographs of (a) HA (b) ZnHA nanopowders

The BET surface area of HA and ZnHA nanopowders as determined from BET analysis is reported in Table 3. HA showed maximum BET surface area amongst all the nanopowders. ZnHA2 and ZnHA10 showed higher BET surface area than ZnHA5 and ZnHA15.

TABLE 3. BET SURFACE AREA OF HA AND ZNHA NANOPOWDERS

Sample	HA	ZnHA2	ZnHA5	ZnHA10	ZnHA15
BET surface area (m^2/gm)	205	189	95	171	66

Phase Analysis and Crystallinity of Nanopowders

The XRD patterns of HA, ZnHA2, ZnAH5, ZnHA10 and ZnHA15 nanopowders are presented in Fig. 2. The XRD patterns matched with JCPDS card no. 09-
432 for hydroxyapatite. The peaks became broader with increasing Zn percentage. The peaks attributable to (2 1 1), (1 1 2) and (3 0 0) reflections merged on increasing the Zn amount. Broadening of (0 0 2), (2 1 1) and (3 1 0) diffraction peaks indicated lower crystallinity for ZnHA nanopowders as compared to HA nanopowder. The lattice parameters 'a' and 'c' for ZnHA2 were higher than HA (Table 4). Both 'a' and 'c' showed gradual decrease in their value up to 10% Zn. ZnHA15 showed increase in 'a' value no change in 'c' value.

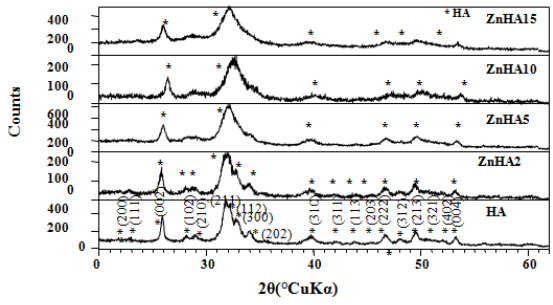

Fig. 2. XRD patterns of HA and ZnHA nanopowders

FTIR Analysis of HA and ZnHA Nanopowders

Fig. 3 shows that the FTIR spectra of ZnHA nanopowders exhibited lower peak intensities than HA nanopowder. The relative intensities for hydroxyl
and phosphate groups decreased with increase in Zn

Table 4. Lattice parameters of HA and ZnHA nanopowders

Sample	Lattice parameters			
	c (Å)	a (Å)	c/a ratio	$V=a^2c\sin(60°)$, Å^3
HA	6.878	9.41	0.731	527.55
ZnHA2	6.895	9.45	0.73	533.34
ZnHA5	6.863	9.34	0.734	518.48
ZnHA10	6.832	9.22	0.74	502.96
ZnHA15	6.832	9.30	0.734	511.89

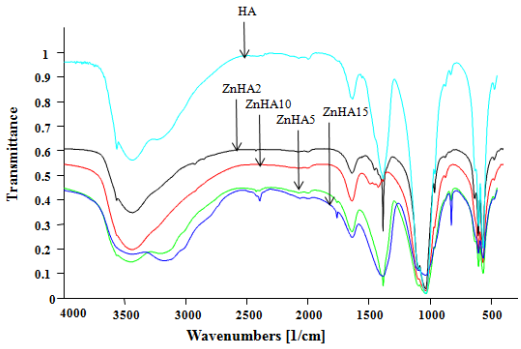

Fig 3. FTIR spectra of HA and ZnHA nanopowders

amount. The decrease in peak intensities at 565, 602 and 1039 cm^{-1} of ZnHA nanopowders with increase in Zn amount reflected lowering of crystallinity. FTIR spectra of HA and ZnHA2 presented the characteristic pattern of hydroxyapatite with a decreased intensity of OH^- vibration modes at 3569 cm^{-1} (stretching) and 630 cm^{-1} (bending) in ZnHA2. This behavior may be associated with Zn incorporation in hydroxyapatite lattice that induces OH^- loss in order to maintain electroneutrality [20, 21]. The characteristic phosphate vibrations of apatite, ν_1 PO_4 (962 cm^{-1}), ν_3 PO_4 (1093-1031 cm^{-1}) and ν_4 PO_4 (569 cm^{-1} and 602 cm^{-1}); hydroxyl vibrations at (3569 cm^{-1}, 630 cm^{-1}) and HPO_4^{2-} vibration (875 cm^{-1}) occurred in ZnHA2 indicating the formation of calcium deficient hydroxyapatite ($Ca_{10-x}Zn_x(PO_4)_6(OH)_2$) or $Ca_{10-x}Zn_x(PO_4)_{6-y}(HPO_4)_y.(OH)_2$. FTIR of ZnHA5 showed elimination of one of the major characteristic peak of OH^- group at 630 cm^{-1} along with HPO_4^{2-} group at 875 cm^{-1}. In FTIR spectra of ZnHA10, OH^- groups at 3569 cm^{-1} and 630 cm^{-1} which are used to characterize the hydoxyapatites, as well as γ_3 phosphate vibration at 1094 cm^{-1} are missing while HPO_4^{2-} group is present. In FTIR spectra of ZnHA15, characteristics peaks of OH^- vibration at 3569 cm^{-1} and 630 cm^{-1} as well as γ_3 phosphate bands at 1094 cm^{-1} are missing. In addition one more peak of PO_4^{2-} i.e 962 cm^{-1} has also gone missing. These changes suggested that increase in Zn amount above 2 mol.% resulted in continuous loss of apatite character. XRD results have also suggested continuous decrease in crystallinity of powders with increase in Zn amount which indicates possibility of formation of amorphous phases like phosphates and hypophosphates of calcium and zinc.

In-vitro Behavior of HA and ZnHA Nanopowders

Fig. 4 shows the variation of pH values as a function of immersion duration for HA and ZnHA nanopowders in SBF up to 30 days. The pH values of the solution for all powders rapidly decreased in the initial stage of immersion test up to two days indicating that Ca ions decreased in SBF leading to the formation of Ca-rich layer on the surface of nanopowders. ZnHA powders showed relatively more decrease in pH than HA. After 2 days, there was an increase in pH value for all powders indicating that PO_4^{2-} ions decrease in SBF leading to Ca-poor layer on the surface of nanopowders. This alternate decrease and increase in pH indicated bioactive behavior of powders. This behaviour continued till the period of present investigation of 30 days. It was observed that variation in pH occurred more frequently in case of ZnHA than HA, indicating more bioactive behavior of ZnHA than HA.

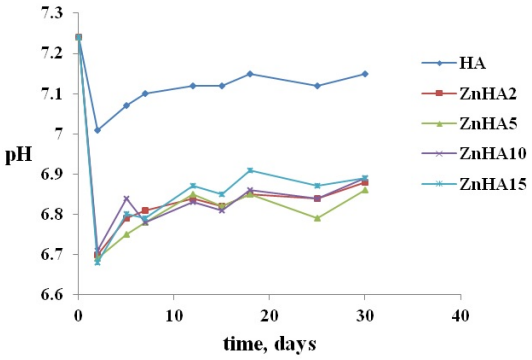

Fig. 4. pH variation of HA and ZnHA in SBF with time

IV.CONCLUSION

Nanodimensional HA and zinc substituted HA have been successfully synthesized using sol-gel technique. Though 1.4, 2.9, 6.1 and 13.1 mol.% of Zn could be incorporated into ZnHA powder synthesized
by adding 2, 5, 10 an 15 mol.% Zn respectively, but
its substitution at Ca sites in apatite structure is limited. This leads to the loss of apatite character of ZnHA powders. The crystallinity of sample decreased with an increase in Zn amount. Zn addition affects the stoichiometry of HA, causing decrease in lattice parameter 'a' and 'c' upto 10 mol.% Zn with increase in 'a' but no change in 'c' for 15 mol.% Zn.

REFERENCES

[1] L.H. Tasker, G.J. Sparey-Taylor, L.D. Nokes, 'Applications of Nanotechnology in Orthopaedic', Clinical Orthopaedic Related Research, 2007, Vol.456, pp. 243-249.

[2] M.P. Ginebra, F.C.M. Driessens, J.A. Planell, 'Effect of the Particle Size on the Micro and Nanostructural Features of Calcium Phosphate Cement: A Kinetic Analysis', Biomaterials, 2004, Vol.25, pp. 3453-3462.

[3] J. Oveson, B. Moller-Madsen , J.S. Thomsen, G. Danscher, L.I. Mosekilde, 'The positive effect of zinc on skeletal strength in growing rats', Bone, 2001,Vol. 29, pp. 565-70.

[4] S. L. Hall, H.P. Dimai, J.R. Farley, 'Effect of zinc on human skeletal alkaline phosphatase activity in vitro', Calcified Tissue International, 1999, Vol. 64, pp. 163-72.

[5] A.S. Parasad, 'Zinc an overview', Nutrition, 1995, Vol.11, pp. 93-95.

[6] M. Yamaguchi, 'Role of zinc in bone formation and bone resorption', Journal of Trace Elements in Experimental Medicine, 1998, Vol.11, pp. 119-35.

[7] A. Bigi, E. Foresti, M. Gandolfi, M. Gazzano, N. Roveri, 'Isomorphous substitutions in b-tricalcium phosphate: the different effects of zinc and strontium', Journal Inorganic Biochemistry, 1997, Vol. 66 pp. 259-65.

[8] N. Kanzaki, K. Onuma, G. Treboux, S. Tsutsumi, A. Ito, 'Inhibitory effect of magnesium and zinc on crystallization kinetics of hydroxyapatite (0 0 0 1) face', Journal of Physical Chemistry B, 2000, Vol. 104, pp. 4189-94.

[9] J. Webb, D.J. Macey, S. Mann, 'Biomineralization of iron in molluscan teeth'. In: Biomineralization: Chemical and Biochemical Perspectives. Mann S, Webb J, Williams RJP, editors. VCH Publishers, 1989, pp. 345-88.

[10] R. Z. LeGeros, M.M. Taheri, G. B. Quirologico, J.P. LeGeros, 'In: Proceedings of the 2nd international phosphorus conference. Boston, Paris: IMPHOS; 1989.

[11] R. Z. LeGeros, J.P. LeGeros, 'Dense hydroxyapatite', An introduction to bioceramics, Singapore: World Scientific, 1993, Vol. 1.

[12] F. Miyaji, Y. Kono, Y. Suyama, 'Formation and structure of zinc-substituted calcium hydroxyapatite', Material Research Bulletin, 2005, Vol.40, pp. 209-20.

[13] S. Hayakawa, K. Ando, K. Tsuru,A. Osaka, 'Structural characterization and protein adsorption property of hydroxyapatite particles modified with zinc ions', Journal of Amercian Ceramic Society, 2007, Vol.90, pp. 565-569.

[14] M. O. Li, X. Xiao, R. Liu, C. Che, L. Huang, 'Structural characterization of zinc-substituted hydroxyapatite prepared by hydrothermal method', Journal of Material Science: Materials in Medicine, 2008, Vol. 19, pp. 797-803.

[15] F. Ren, R. Xin, W. Ge, Y. Leng, 'Characterization and structural analysis of zinc- substituted hydroxyapatite', Acta Biomaterialia, 2009, Vol.5, pp. 3141-3149.

[16] R. Joseph and K.E. Tanner, 'Effect of Morphological Features and Surface Area of Hydroxyapatite on the Fatigue Behavior of Hydroxyapatite- Polyethylene Composites', Biomacromolecules, 2005, Vol.6, pp. 1021-1026.

[17] L. Clausen and I. Fabricius, 'BET measurements: Outgassing of minerals', Journal of Colloid and Interface Science, 2000, Vol.227, pp. 7-15.

[18] T.J. Webster, E. A. Massa-Schlueter, J. L. Smith, E. B. Slamovich, 'Osteoblast response to hydroxyapatite doped with divalent and trivalent cations', Biomaterials, 2004, Vol.25, pp. 2111-2121.

[19] T. Kukubo, 'Formation of bone-like apatite on metals and polymers by a biomimetic process', Biomaterials, 1996, Vol. 12, pp.155-163.

[20] C. M. Botelho, M. A. Lopes I. R., Gibson, S. M. Best, J. D. Santos, 'Structural Analysis of Si-Substituted Hydroxyapatite: Zeta Potential and X-Ray Photoelectron Spectroscopy', Journal of Material Science: Materials in Medicine, 2002, Vol.13, pp. 1123-27.

[21] D. Acros, J. Carvajal, M. R Vallet-Regi, 'Silicon incorporation in hydroxyapatite obtained by controlled crystallization', Chemistry of Materials, 2004, Vol.16, 2300-2308.